



## COVER SHEET

---

**This is the author-version of a conference paper published as:**

Aktarujjaman, M. and Kashem, M.A. and Negnevitsky, M. and Ledwich, Gerard (2006) Smoothing Output Power of a Doubly Fed Wind Turbine with an Energy Storage System . In *Proceedings Australian Universities Power Engineering Conference 2006*, Melbourne, Victoria, Australia.

**Copyright 2006 (please consult author)**

Accessed from <http://eprints.qut.edu.au>

# Smoothing Output Power of a Doubly Fed Wind Turbine with an Energy Storage System

M.Aktarujjaman, M.A. Kashem, M. Negnevitsky  
School of Engineering  
University of Tasmania  
Tasmania, Australia  
mda0@utas.edu.au

G. Ledwich  
School of Engineering Systems Queensland  
University of Technology Brisbane,  
Australia

## ABSTRACT

*Wind energy sources are characterized by irregularity and unpredictability. In normal operation, random properties of wind and blade rotational turbulence can produce unwanted fluctuation on the voltage and power supplied into the system. Power output of a wind turbine is a function of wind speed. Wind turbine is a source of power fluctuations due to the nature of wind speed. This fluctuating power will have its impact on power balance and voltage at the point of common coupling. Small variation of wind speed could cause a large variation in the extracted power. As a result, large voltage fluctuation may result in voltage variations outside the regulation limit at connection point. In this paper, a method has been developed to reduce output power fluctuations of a wind turbine with an energy storage system using stator side converter. The developed method has been tested through modelling a doubly fed wind turbine and a battery storage system, using SimPowerSystems tools of MATLAB and simulated for operation as a grid connected system.*

## 1. INTRODUCTION

Renewable energy resources are promising generation sources for power provider due to advance technology, low production cost, and environmental friendly. Furthermore, cost of fossil fuel is driving force for choosing energy production from renewable energy resources such as wind, solar, biomass etc. Among them wind power has been considered as a strong alternative for traditional power system. Advance turbine technology has reached in range of multi MW age. Multi MW generation capabilities of wind power with better control (Doubly Fed Induction Generator, DFIG) can increase the contribution of renewable energy into the power grid.

Wind energy source is characterised by irregularity and unpredictability. Average wind power is a function of wind speed and the speed of wind is a random process. Furthermore, during normal operation, blade rotational turbulence and tower shadow also produce fluctuation into the mechanical torque. Due to those facts, wind turbine is a source of fluctuating torque, which is responsible for producing unwanted fluctuations of the power supplied into the Point of Common Coupling (PCC). Wind power is often associated with power variation and power fluctuation. In addition, a favourable location of wind source is often located far from traditional power generation or strong grid. Wind power generation is often connected to a weak grid. A weak grid is poorly interconnected, far from main generation unit or isolated or has relatively low spinning reserves [1], with long line and limited power exporting capabilities. In a weak system or an isolated system, the

response of the system voltage and frequency are highly sensitive to the power generation and consumption. Fluctuate power can often cause the violation of voltage and frequency limits in the weak system. Fluctuating power also causes an unwanted start-stop cycle of secondary generating stations such as diesel generators [2].

Wind turbine's inertia can compensate a certain amount of power fluctuation. However, when a wind turbine is feeding power to a small grid or a stand alone load, this power fluctuation can be a severe problem for the system stability. Energy storage can provide a faster active power compensation to reduce the power fluctuations and flicker. The response of the output power of wind turbine with storage is more robust. A storage system can rapidly compensate active power to the system. This eliminates the impact of fluctuation from wind gust and keeps the output power of wind turbine more stable for the grid.

Different wind generation technologies are available in market. Among them Doubly Fed Induction Generator (is an attractive option because of allows the variable speed operation, control of the real and reactive power, and reduced rating of a converter [3]. The main improvement of a recent configuration with a storage system in the DC link is providing an extra spinning reserve facility for the wind system, which can be used for sink or source of active power. Theoretically, the storage system has the capability to compensate enough real power to the system for smoothing instantaneous fluctuations of wind or loads [4].

In this paper, the key elements of power fluctuation of the wind turbine have been discussed and identified. The control behaviour of the DC link energy storage system has been modelled and observed. Also the improvement of the system has been simulated and results are presented.

## 2. PROBLEM STATEMENT

During normal operation conditions, random properties of wind, tower shadow and blade rotational turbulence can produce unwanted fluctuation on the mechanical torque. This fluctuating torque is responsible for fluctuating the real power of the generator, which is a function of the mechanical torque. In a weak system, positive feedback occurs between the power fluctuation and the voltage fluctuation with respect to the same input torque and so the power fluctuation may also increase [5]. Fluctuating input torque makes this scenario even more severe in absence of an appropriate compensator.

The rate of the wind speed-change is proportional to the unwanted power variations and fluctuations for the load in a stand alone system or a weak grid. Due to those facts, a wind turbine can be considered as a source of active and reactive power fluctuations. In a large wind power generation unit (> 1 MW), even a small variation of the wind speed can cause a large variation in the power generated.

The total output power of a wind generator can be explained as below:

$$P = P_{base} \pm \Delta P \quad (1)$$

The total output power of the wind turbine is a combination of the base power and the power fluctuation caused by the wind speed, tower shadow and blade rotational speed.  $P_{base}$  is the fluctuation free mean power.

The fluctuating power can be expressed in the form of the fluctuating torque and slip as follows [5]:

$$\Delta P = \Delta T_m - h \frac{d}{dt} \Delta s \quad (2)$$

Where  $h = \omega \frac{J \left( \frac{\omega}{p} \right)^2}{S_n}$  = inertial constant;  $\Delta P$  = Fluctuating

power;  $\Delta T_m$  = Fluctuating torque;  $\Delta s$  = Fluctuating slip;  $J$  = Moment of inertia;  $\omega$  = Angular velocity (rad/sec);  $p$  = Number of pole pairs;  $S_n$  = Rated capacity (VA);

In Eq. (2), it is seen that the fluctuating torque and fluctuating slip are the key contributors for creating an unwanted power fluctuation in the output power. The power fluctuation has its own magnitude and frequency, which depends on the rate of change of the wind speed.

### 3. SYSTEMS AND COMPONENTS MODELLING

The system consists of a DFIG with dc-ac and ac-dc converters, battery storage, loads and grid. The generator uses a wound-rotor induction machine where the rotor terminals are fed via a back-to-back PWM voltage source converter [6-7]. The control system is able to control real and reactive power independently. The rotor side converter is responsible for controlling the speed of the generator and stator reactive power, while the stator side converter will controls the fluctuating power supply and may also be used to supply reactive power to the system.

Fig.1 shows a typical arrangement of a DFIG equipped with a wind turbine and a battery storage system connected to the DC link of the back to back PWM converter. The stator side converter controls the instantaneous real power exchange between the stator and the storage system.

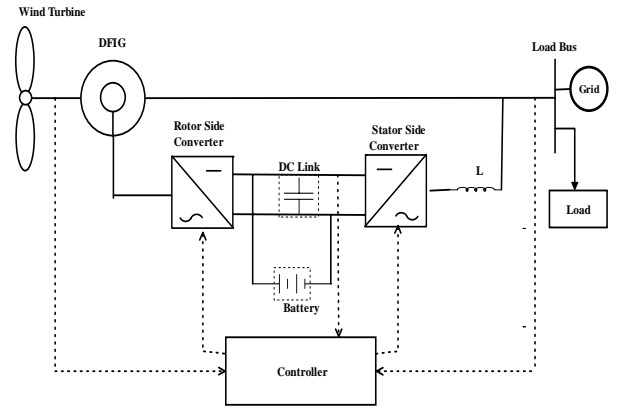


Fig.1. Diagram of DFIG wind turbine with storage system

Storage controller receives control signals from the available wind energy and the grid system. The state of charge of the storage system also plays major role on the storage participation of the system mode of operation. The storage system provides instantaneous active power compensation through the stator side converter to the turbine output power as well as the DC link voltage stabilisation.

### 3.1. WIND TURBINE MODEL

Wind turbine is a non-linear system whose output depends on optimal values of various parameters. Total power of a wind turbine can be defined as [8]:

$$P_{wind} = 0.5 \rho A_r v^3 \quad (3)$$

where  $\rho$  is the air density [ $\text{kg}/\text{m}^3$ ],  $A_r$  is the area swept by the rotor and  $v$  is the wind speed. The wind power output is given by the power curve, depending on the wind speed, which is expressed as

$$P_{wind} = \begin{cases} P_{rated} & \text{for } v_i < v \leq v_o \\ P(v) & \text{for } v_i < v \leq v_r \\ 0 & \text{for } v_i > v > v_o \end{cases}$$

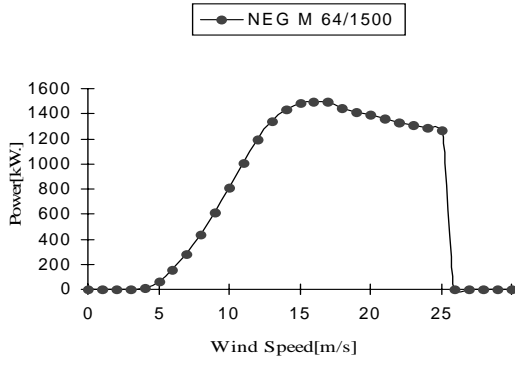
where  $v_i$ ,  $v_r$  and  $v_o$  are the cut-in, rated and cut-off wind speed, respectively. The function,  $P(v)$ , describes the wind power between cut-in wind speed and rated wind speed. The mechanical power of wind turbine can be determined by [8]:

$$P_{mech} = P_{wind} C_p(\lambda, \beta) \quad (4)$$

where  $C_p$  is the performance coefficient and is a function of the tip speed ratio and pitch angle. The tip speed ratio is the ratio of the speed at the tip of the blades to the speed of the wind and can be defined as [8]:

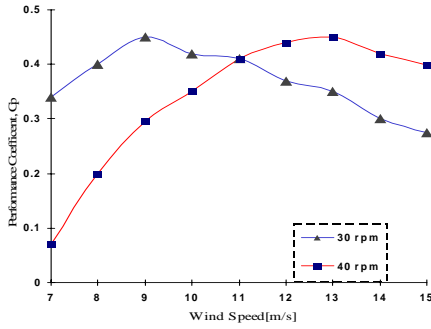
$$\lambda = \frac{\omega R}{v} \quad (5)$$

Fig.2 shows a typical power curve of commercially available wind turbine [8]:



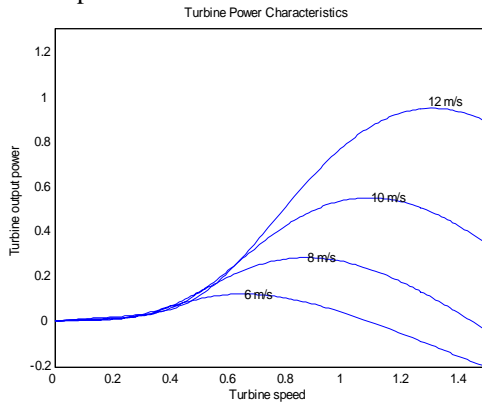
**Fig.2:** power curve of wind turbine

Fig. 3 shows performance coefficients,  $C_p$  for two different wind speeds. As it can be seen that initially the wind speed increases, the value of performance coefficient also increases. If the wind speed increases further than the value at the maximum performance coefficient, the performance coefficient  $C_p$  will decrease. This characteristics makes the wind turbine self-regulating its output power by operating at lower efficiency for high wind speed. It also shows that higher efficiency can be obtained on low wind speed and for low rpm of the rotor blade [8]:



**Fig.3:** Cp-wind speed curve of wind turbine

The performance coefficient,  $C_p$ , of a wind turbine varies with wind speed. Fig.4 shows the power characteristic curve of the wind turbine for different wind speeds.



**Fig.4:** Turbine Power Characteristics

### 3.2. DOUBLY FED INDUCTION GENERATOR (DFIG) MODEL

Direct and quadrature axes (d-q) representation of the DFIG is used for analysis, simulation and control. The equations of the asynchronous machine in the d-q reference frame are [10-11]:

$$\begin{cases} V_{sd} = R_s I_{sd} + \frac{d\phi_{sd}}{dt} - \omega_s \phi_{sq} \\ V_{sq} = R_s I_{sq} + \frac{d\phi_{sq}}{dt} + \omega_s \phi_{sd} \\ V_{rd} = R_r I_{rd} + \frac{d\phi_{rd}}{dt} - \omega_r \phi_{rq} \\ V_{rq} = R_r I_{rq} + \frac{d\phi_{rq}}{dt} + \omega_r \phi_{rd} \end{cases} \quad (6)$$

where stator and rotor fluxes are expressed in function of the current by:

$$\begin{cases} \phi_{sd} = L_s I_{sd} + L_m I_{rd} \\ \phi_{sq} = L_s I_{sq} + L_m I_{rq} \\ \phi_{rd} = L_r I_{rd} + L_m I_{sd} \\ \phi_{rq} = L_r I_{rq} + L_m I_{sq} \end{cases} \quad (7)$$

Where

- $V_s, V_r$  : stator and rotor voltage;
- $I_s, I_r$  : stator and rotor current;
- $L_s, L_r$  : stator and rotor self inductance;
- $L_m$  : mutual inductance;
- $R_s, R_r$  : stator and rotor resistances;
- $\phi$  : flux linkage;
- $\omega$  : Angular velocity (rad/sec);

From the equations for the rotor fluxes,  $\phi_{rd}$  and  $\phi_{rq}$ , the following expressions for the rotor currents  $I_{rd}$  and  $I_{rq}$  are derived [11]:

$$I_{rd} = \frac{\phi_{rd} + L_m I_{sd}}{L_r}, \quad I_{rq} = \frac{\phi_{rq} + L_m I_{sq}}{L_r} \quad (8)$$

In the generating mode, we obtain

$$\begin{cases} V_{sd} = -R_s I_{sd} + \omega_s L_s I_{sq} - \omega_s L_m \left( \frac{\phi_{rq} + L_m I_{sq}}{L_r} \right) \\ V_{sq} = -R_s I_{sq} - \omega_s L_s I_{sd} + \omega_s L_m \left( \frac{\phi_{rd} + L_m I_{sd}}{L_r} \right) \end{cases} \quad (9)$$

Rearranging the above equations, the stator voltage can be expressed as a function of the voltage behind transient reactance by [11]:

$$\begin{cases} V_{sd} = -R_s I_{sd} + X' I_{sq} + e_d \\ V_{sq} = -R_s I_{sq} - X' I_{sd} + e_q \end{cases} \quad (10)$$

The synchronous reactance and transient reactance are defined as

$$X = \omega_s L_s, \quad X' = \omega_s \left( L_s - \frac{L_m^2}{L_r} \right) \quad (11)$$

$e_d$  and  $e_q$  are respectively the direct and quadrature components of the voltage behind transient reactance, and can be defined as

$$e_d = -\frac{\omega_s L_m}{L_r} \phi_{rq}, \quad e_q = \frac{\omega_s L_m}{L_r} \phi_{rd} \quad (12)$$

$$\text{where, } \phi_{rd} = \frac{L_r}{\omega_s L_m} e_q, \quad \phi_{rq} = -\frac{L_r}{\omega_s L_m} e_d \quad (13)$$

Substituting Eqs. (8) and (13) into the equation (6) for the rotor voltage, we obtain [11]:

$$\begin{aligned} V_{rd} &= R_r I_{rd} + \frac{d\phi_{rd}}{dt} - \omega_r \phi_{rq} \\ &= R_r \left( \frac{\phi_{rd} + L_m I_{sd}}{L_r} \right) + \frac{d\phi_{rd}}{dt} - s\omega_s \phi_{rq} \\ V_{rq} &= R_r I_{rq} + \frac{d\phi_{rq}}{dt} + \omega_r \phi_{rd} \\ &= R_r \left( \frac{\phi_{rq} + L_m I_{sq}}{L_r} \right) + \frac{d\phi_{rq}}{dt} + s\omega_s \phi_{rs} \end{aligned} \quad (14)$$

Taking the derivatives for  $e_d$  and  $e_q$  we get

$$\left. \begin{aligned} \frac{d}{dt} e_d &= -\frac{1}{t_{os}} \left[ e_d - (X - X') I_{sq} \right] - \omega_s \frac{L_m}{L_r} V_{rq} + s\omega_s e_q \\ \frac{d}{dt} e_q &= -\frac{1}{t_{os}} \left[ e_q - (X - X') I_{sd} \right] + \omega_s \frac{L_m}{L_r} V_{rd} - s\omega_s e_d \end{aligned} \right\} \quad (15)$$

The transient open circuit time constant is defined as [11]:

$$t_{os} = \frac{L_r}{R_r} \quad (16)$$

From Eq.(15), the general form of the derivative is

$$\frac{d}{dt} e = -\frac{1}{\omega_s t_s} \left[ e - (X - X') I_s \right] - j\omega_s \frac{L_m}{L_r} V_r + js\omega_s e \quad (17)$$

At steady state,  $\frac{d}{dt}(e) = 0$ , Eq.(17) will become

$$0 = -\frac{1}{\omega_s t_s} \left[ e - (X - X') I_s \right] - j\omega_s \frac{L_m}{L_r} V_r + js\omega_s e \quad (18)$$

In Eq. (18), for normal operating values of  $s$ , the divider term is small compared with the final two terms. So, the Eq.(18) can be reduced to the following form.

$$\frac{L_m}{L_r} V_r \cong se \quad (19)$$

The ratio between the mutual and rotor reactance is usually close to the unity. Thus the rotor voltage is approximately the product of the internal voltage and the slip. Hence, the magnitude of the internal voltage is slightly varies. The magnitude and sign of the rotor voltage is approximately proportional to the magnitude of the slip [11].

Fig.5 shows the normal operating conditions of the DFIG [11]. In the sub-synchronous operation mode, slip is positive, the rotor voltage is in phase with the internal voltage,  $e$ .

In the super-synchronous operation mode, slip is negative, the rotor voltage is the anti-phase with the internal voltage  $e$ .

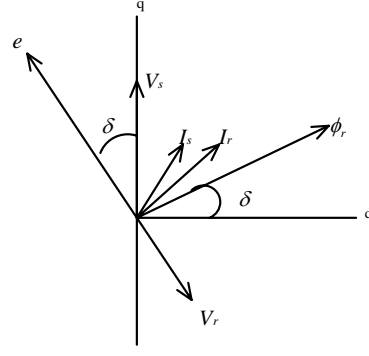


Fig.5: Vector representation of the DFIG

The DFIG torque in per unit can be expressed as voltage behind reactance as follows [11].

$$T_e = \frac{e_d I_{sd} + e_q I_{qs}}{\omega_s} \quad (20)$$

It can be also expressed as a function of air-gap flux and rotor current [10].

$$T_e = \frac{3p}{22} |\phi_{dqm}| |i_{rdq}| \sin \delta \quad (21)$$

where  $\phi_{dqm} = \phi_{sdq} - i_{sdq} L_s$  and  $\phi_{dqm} = \phi_{rdq} - i_{rdq} L_r$

### 3.3. TORQUE CONTROL

In Eq. (21),  $\delta$  (torque angle) is the angle between the air gap flux and rotor current vectors seen in the synchronous reference frame. With the alignment of the air gap flux to the d-axis of the reference frame, we will have [10]

$$\phi_{dqm} = \phi_{dm} \quad \text{and} \quad \phi_{qm} = 0$$

Then, the torque equation is reduced as a function of the q-axis component of the rotor current [10,11]:

$$\begin{aligned} T_e &= \frac{3p}{22} |\phi_{dm}| |i_{rq}| \sin \delta \\ &= \frac{3p}{22} (\phi_{dm} i_{rq} - \phi_{qm} i_{rd}) \end{aligned} \quad (22)$$

The electromechanical torque can be viewed as the result of the interaction between rotor current and air gap flux, regardless of the selection of the reference frame. The q-axis component of rotor current can be used to control the torque of the generator.

### 3.4. REACTIVE POWER CONTROL

Reactive power of the DFIG can be controlled through the rotor current vector to realize unity or leading power factor operation. Assuming that the required reactive power to the stator is  $Q_s$ , which can be expressed as a function of the d-axis component of the rotor current by [10,11]:

$$Q_s = \frac{3}{2} \omega_s (v_{sq} i_{sd} - v_{sd} i_{sq}) \quad (24)$$

If the air gap flux is constant then the reactive power can be controlled by controlling the d-axis component of the rotor current  $i_{dr}$ . For reactive power control, the rotor speed and the rotor position must be known for the rotor current vector projection [10].

### 3.5. STATOR SIDE AND ROTOR SIDE CONVERTER

Stator Side Converter (SSC) is used to control the required real power for smoothing the output power. Reference power is compared with generator output power. Then P-I controller is responsible for producing current reference for inner current control loop, which is then compare with the d-axis component of line current. P-I controller is used for regulation.

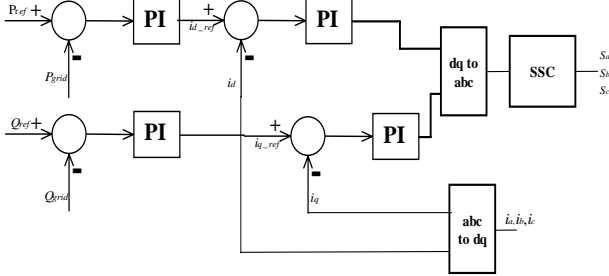


Fig. 6: Stator Side Converter Controller

According to the system requirement, reactive power can be controlled through reactive power control loop as shown in Fig. 6. In reactive power control, the measured reactive power is compared with the reference reactive power, and the PI controller produces the q-axis component of the current reference for the inner current control loop. The PI controller is used for regulating the difference. The storage system is used for stabilising the DC link voltage with storage limitation.

The control of the Rotor Side Converter (RSC) is vary much similar with the control given [6-7]. The control system is responsible for creating enough air gap flux through injecting the rotor current to meet the real and reactive power requirements of the system.

### 3.6. STORAGE SYSTEM

The purpose of the energy storage is to smooth the stochastic wind variations in order to obtain firm power output to DFIG. If the wind power output exceeds the desired level, the excess power is used to charge the storage through stator side converter. Stored energy can be used when wind power output is less than desired level.

The charging and discharging power of the energy storage system can be calculated on the basis of available wind power output as follows [12]:

$$P_{dch} = \begin{cases} P_d - P_w & \text{for } P_w \leq P_d \\ 0 & \text{for } P_w > P_d \end{cases} \quad (25)$$

$$P_{ch} = \begin{cases} P_w - P_d & \text{for } P_w > P_d \\ 0 & \text{for } P_w \leq P_d \end{cases} \quad (26)$$

where  $P_{ch}$ ,  $P_{dch}$ ,  $P_d$ , and  $P_w$  are the charging, discharging, desired and actual wind power, respectively.

The energy storage system can be characterised by its charging efficiency  $\eta_{ch}$  and discharging efficiency  $\eta_{dch}$  as follows [12]:

$$E_{ch} = \eta_{ch}(P_{ch}) \cdot P_{ch} \quad (27)$$

$$E_{dch} = \frac{P_{dch}}{\eta_{dch}(P_{dch})} \quad (28)$$

where  $E_{ch}$  and  $E_{dch}$  are the stored and discharged energy respectively. In the case of charging and discharging system with 100% efficient, the stored energy will be equivalent to the charging and the discharged energy and the charging power will be the same as the discharging power.

The rating of the storage system must be less than the converter's rating. The voltage across the storage system would vary roughly within  $\pm 10\%$  of the DC link voltage, depending on the amount of energy stored. The size of the storage size for DFIG can be calculated as [3]:

$$E = P_{conR} \cdot P_{rated} \cdot t \quad (29)$$

$$E = \frac{1}{2} C (V_{max}^2 - V_{min}^2) \quad (30)$$

where  $E$ ,  $C$ ,  $P_{conR}$ ,  $P_{rated}$ ,  $V_{max}$  and  $V_{min}$  are the stored energy, capacitor, converter power ratings, machine's rated power, maximum and minimum DC link voltages, respectively. The capacitor value can be calculated as follows:

$$C = \frac{2P_{conR} \cdot P_{rated} \cdot t}{(V_{max}^2 - V_{min}^2)} \quad (31)$$

Capacitor is the key element of the storage system. Eq. (31) can be used to identify the value of the capacitor for the energy storage system.

## 4. SIMULATION RESULTS AND DISCUSSION

Simulation has been carried out using MATLAB SimPowerSystems. Three cases have been investigated and results are presented. All simulations are run with the 500 sec duration with the same wind variation. Wind model speed varies within the 8-12 m/s speed range. Large amount of capacitor is used for modeling of a storage system. A 9 MW wind firm is connected with the grid. The wind firm consists of  $6 \times 1.5$  MW DFIG wind turbines. Simulation results show the effectiveness of DFIG in the sub-synchronous and super synchronous speed of operations. Investigations are conducted on the effect of the storage system. The following responses are examined: wind power output, DC link voltage, Power of Stator Side Converter (SSC), Power of Rotor Side Converter (RSC), Generator speed, and wind speed.

In the system without any storage, Fig.7 shows the responses and behaviors of the turbine output and the controller during the wind variation. Fig. 7 (a) shows the variation of wind power. The minimum power is exported to the system is approximately 2.25 MW in the low wind speed situation whereas the maximum power is approximately 6 MW. Most of the power variation is seen between 3 MW and 4 MW. Fig. 7(b) shows the variation of DC link voltage. The stabilisation of DC link voltage depends on the quick power exchanging capability of SSC. Figs 7(c) and 7(d) show the power exchanging behavior of two back-to-back PWM

converters. Fig.7(c) shows that the SSC is exchanging power between the DFIG stator terminal and the DC link for stabilizing DC link voltage. With the response of power taking or feeding by the RSC, DC link faces over and under voltage situation. DC link voltage has to be stabilized by the SSC. SSC provides instant support for the DC link with help of DFIG stator power. As a result, wind output power faces more power variation. Fig.7 (d) shows that the RSC is exchanging power between the DFIG rotor and the DC link for helping to build enough air gap flux for DFIG in the generating mode of operation. The generator speed shown in Fig.7 (e) is largely affected by the variation of wind speed shown in Fig.7 (f). It is seen that the wind variation lies between 7 m/s and 13 m/s. Variation effect of the generator speed can be found in the output of the wind power shown in Fig. 7 (a), which is also varying.

A storage system ( $C=10000$  F) is connected in the DC link. Fig.8 shows the responses and behaviors of the DFIG output and the controller during the wind variation. It is seen in Fig. 8 (a) that the variation of wind output power is comparatively smoother than the system without storage arrangement shown in Fig. 7 (a). The variation of DC link voltage (Fig. 8 (b)) is also less compared to Fig. 7 (b). The power exchanging behaviors of the SSC and RSC are shown in Figs 8 (c) and 8 (d). The power exporting and importing of SSC to and from the DFIG stator terminal is smoother than Fig. 7(c), which prevents the rapid changing behavior of the power output of the DFIG stator terminal. Frequent power taking and feeding by the SSC may create more power fluctuation for the output power. In this arrangement, SSC's power exchanging behavior has delayed significantly than the behavior shown in Fig.7 (c). Furthermore, the stabilization of DC link voltage has improved. Figs 8 (e) and 8(f) show the generator speed and wind speed are similar to 7 (e) and 7(f) respectively, because test has been conducted with the same wind variation.

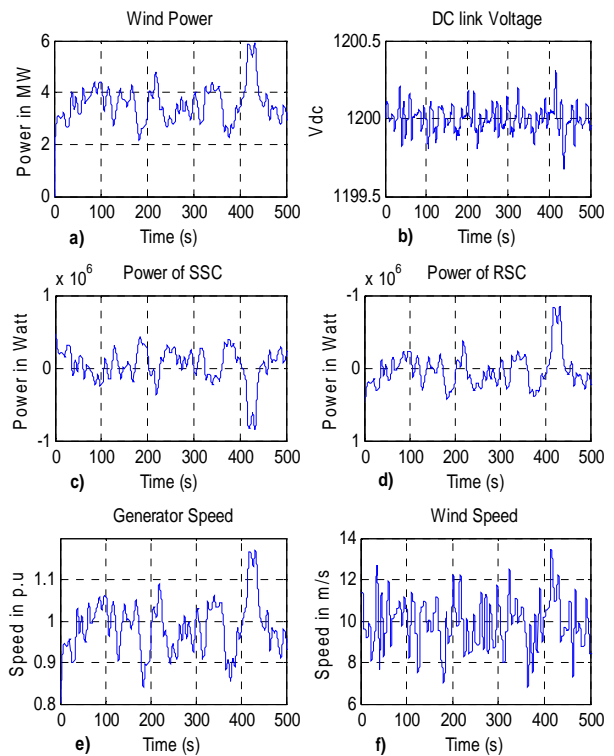


Fig.7: Responses of DFIG without storage system, a) wind power, b) DC link Voltage, c) Power of SSC, d) Power of RSC, e) Generator rotor speed, f) wind speed.

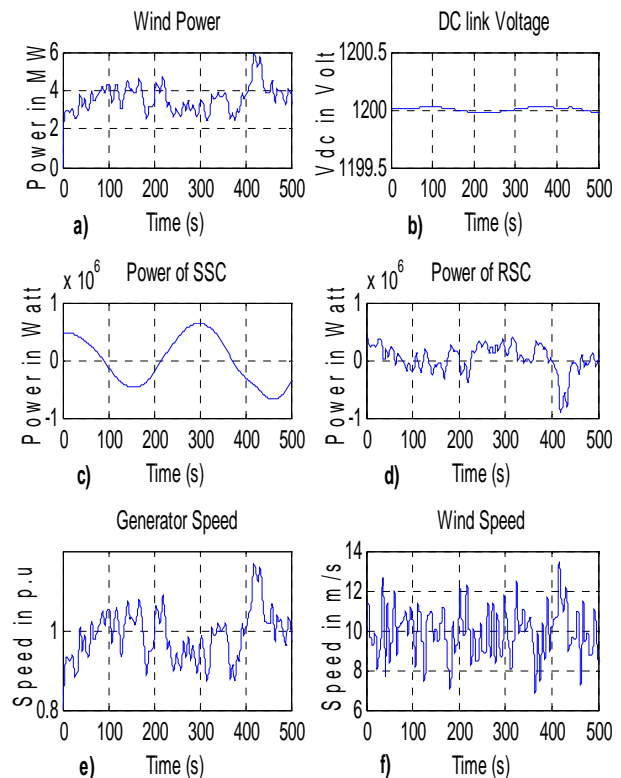


Fig.8: Responses of DFIG with storage system a) wind power, b) DC link Voltage, c) Power of SSC, d) Power of RSC, e) Generator rotor speed, f) Wind speed.

Next, a large storage system ( $C=1000000F$ ) is connected with the DC link. Fig.9 shows the responses and behaviors of the DFIG output and controller during the same wind variation. The output wind power in Fig.9 (a) is smoother than the case shown in Fig. 7(a) and Fig. 8(a). Fig. 9 (b) shows that the energy storage system stabilises the DC link voltage significantly. SSC's steady operation will provide more firm power to the grid. Figs 9 (c) and 9(d) show the behaviour of SSC and RSC with large energy storage system during wind variation. The variation of wind speed and the responses of the generator speed are shown in Figs 9(f) and 9(e), respectively.

Fig. 10 shows overall view of the energy storage effect on the DFIG power output. In Fig.10, three curves show that the nature of output power of the wind turbine without storage and the improvement of power smoothing using storage for the same wind variation.

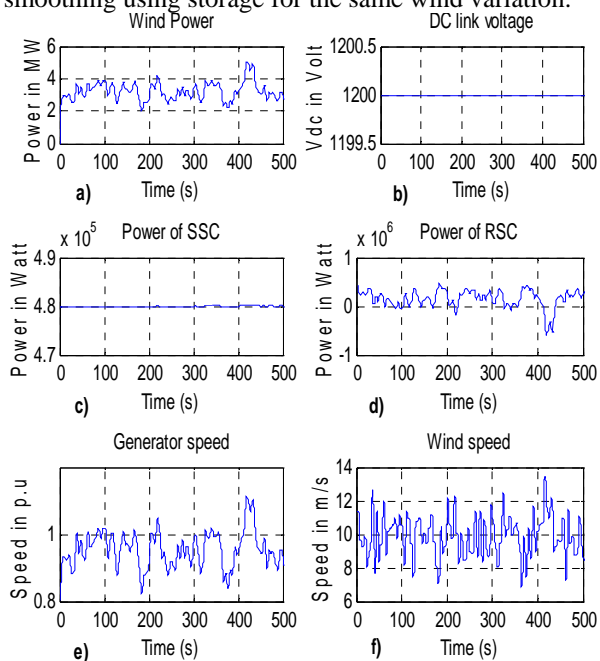


Fig.9: Responses of DFIG with large storage system a) wind power, b) DC link Voltage, c) Power of SSC, d) Power of RSC, e) Generator rotor speed, f) Wind speed.

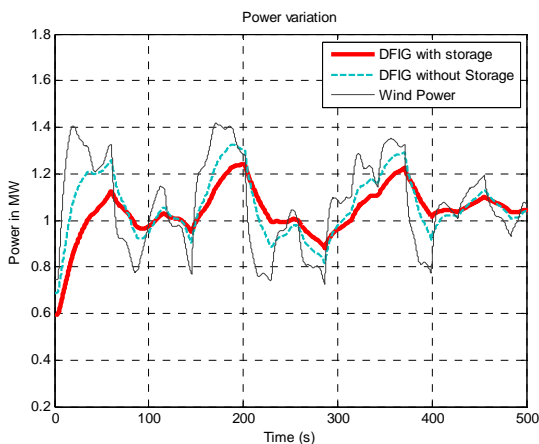


Fig.10: Power variation curve for DFIG with and without storage

## 5. CONCLUSIONS

In this paper, power smoothing capability of a DFIG with energy storage system in the DC link has been investigated with the help of SimPowerSystem toolbox of MATLAB. Using same stator side converter of DFIG will eliminate the need of an extra converter for the energy storage system and reduce the system cost significantly. The control system in the proposed arrangement of DFIG is able to reduce power fluctuation with help of storage system. The results show the enhancement of power quality and the ability of the storage system to produce more clean power to the grid system. It also provides more system reliability due to the capability of providing instantaneous real power for the system. It can reduce the negative impact of stator side converter's power import and export from the stator terminal of DFIG and ensure maximum power extraction from the wind and deliver to the system.

## 6. ACKNOWLEDGEMENTS

This research has been funded by the Australian Research Council under ARC Linkage Grant K0014223 "Integration of Distributed and Renewable Power Generation into Electricity Grid Systems". The authors also would like to thank Aurora Energy, Tasmania for their support.

## REFERENCES

- [1] O.A.M. Alejandro, "Issues Regarding the Integration of Induction Wind Turbines in Weak Electrical Networks", Nordic Wind Power Conference, 1-2 March, 2004.
- [2] R. Cardenas, R. Peña, G. M. Asher, J. Clare, and R. Blasco-Gimenez, "Control strategies for power smoothing using a flywheel driven by a sensorless vector-controlled induction machine operating in a wide speed range," *IEEE Trans. Ind. Electron.*, vol. 51, no. 3, pp. 603-614, June 2004.
- [3] C. Abbey and G. Joss, "Integration of Energy Storage with a Doubly-Fed Induction Machine for Wind Power Generation", IEEE PES 2004, Aachen, Germany, July 2004.
- [4] W.R. Lachs, and H. Tabatabaci-Yazdi, "Energy Storage in Power Systems", IEEE Int. Conference on Power Electronics and Drive Systems, PEDs'99, July 1999, pp.843-848.
- [5] Go. Takata, N. Katayama, M. Miyaku, and T. Nanahara, "Study on Power fluctuation Characteristics of Wind Energy Converters with Fluctuating Turbine Torque", *EE in Japan*, vol.153, No.4, 2005, translated from *Denki Gakkai Ronbunshi*, Vol.124-B, No. 10, October 2004, pp.1231-1239.
- [6] A. Miller, E. Muljadi, and D. Zinger, "A Variable Speed Wind Turbine Power Control", *IEEE Trans. On Energy Conversion*, Vol. 12, No. 2, June 1997, pp. 181-186.
- [7] R. Peña, J. C. Clare, and G. M. Asher, "Doubly Fed Induction Generator using back-to-back PWM converters and its application to variable speed wind-energy generation," *Proc. Inst. Elect. Eng., Elect. Power Appl.*, vol.143, no. 3, pp. 231-241, May 1996.
- [8] G.M. Masters, "Renewable and Efficient Electric Power Systems", IEEE press, Wiley-Interscience, Hoboken, New Jersey, 2004.
- [9] Jukka V. Paatero and Peter D. Lund, "Effect of Energy Storage on Variations in Wind Power," *Wind Energy J.*, vol. 8, pp. 421-441, 2005.
- [10] Longya Xu and W. Cheng, "Torque and Reactive power control of a Doubly Fed Induction Machine by Position Sensorless Scheme", *IEEE Trans on Industry Applications*, Vol.31, No.3, May/June 1995, pp.636-642.

- [11] O. Anaya-Lara, F.M Hughes, N. Jenkins and G. Strbac, “ Rotor Flux Magnitude and Angle Control Strategy for Doubly Fed Induction Generator”, Wind Energy, 2006.
- [12] Magnus Korpas, “Distributed Energy Systems with Wind Power and Energy Storage”, Doctoral Thesis, Norwegian University of Science and Technology, Trondheim, Norway,2004.